Acta Crystallographica Section F
Structural Biology and Crystallization Communications
ISSN 1744-3091

Structure of the catalytic domain of the hyperthermophilic chitinase from *Pyrococcus furiosus*

Tsutomu Nakamura,‡ Shouhei Mine,‡ Yoshihisa Hagihara, Kazuhiko Ishikawa and Koichi Uegaki*

National Institute of Advanced Industrial Science and Technology (AIST), Ikeda, Osaka 563-8577, Japan

‡ These authors contributed equally to this work.

Correspondence e-mail: k-uegaki@aist.go.jp

Received 22 September 2006
Accepted 30 November 2006

PDB Reference: archaeal chitinase, 2dsk, r2dsksf.

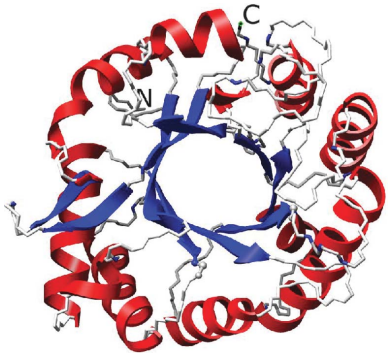

The crystal structure of the catalytic domain of a chitinase from the hyperthermophilic archaeon *Pyrococcus furiosus* ($AD2_{PF\text{-}ChiA}$) has been determined at 1.5 Å resolution. This is the first structure of the catalytic domain of an archaeal chitinase. The overall structure of $AD2_{PF\text{-}ChiA}$ is a TIM-barrel fold with a tunnel-like active site that is a common feature of family 18 chitinases. Although the catalytic residues (Asp522, Asp524 and Glu526) are conserved, comparison of the conserved residues and structures with those of other homologous chitinases indicates that the catalytic mechanism of PF-ChiA is different from that of family 18 chitinases.

1. Introduction

Chitinases (EC 3.2.1.14) hydrolyze chitin, a polymer of β-1,4-linked *N*-acetylglucosamine (GlcNAc), and are classified into two families (families 18 and 19 in the CAZy database; http://afmb.cnrs-mrs.fr/CAZY/) according to amino-acid sequence similarity (Henrissat, 1991). Family 18 chitinases include glycoside hydrolases, which have been found in many organisms ranging from bacteria to humans (Henrissat & Davies, 1997).

The catalytic domains of family 18 chitinases have $(\beta/\alpha)_8$-barrel folds and are characterized by several conserved sequence motifs (Terwisscha van Scheltinga *et al.*, 1996; Suzuki *et al.*, 1999). Three-dimensional structures have been reported for bacterial family 18 chitinases, such as chitinases A and B from *Serratia marcescens* and chitinase A1 from *Bacillus circulans* (Perrakis *et al.*, 1994; van Aalten *et al.*, 2000; Matsumoto *et al.*, 1999). In particular, the catalytic mechanism of chitinase B has been investigated through extensive structure and mutagenesis studies (van Aalten *et al.*, 2001). However, little is known about the structure and function of archaeal chitinases.

In the genome database of the hyperthermophilic archaeon *Pyrococcus furiosus*, we found two adjacent genes (PF1234 and PF1233) homologous to those of the chitinase of *Thermococcus kodakaraensis*. On analysis of the structural gene of *P. furiosus*, it appeared that a nucleotide insertion (the 1006th adenine from the ORF start position) in PF1234 has caused a frame shift and separated the genes. By deletion of the inserted nucleotide in PF1234, the best match was achieved between the chitinases of *T. kodakaraenesis* and *P. furiosus* (Oku & Ishikawa, 2006). This artificial recombinant chitinase (referred to as PF-ChiA) possesses two chitin-binding domains ($ChBD1_{PF\text{-}ChiA}$ and $ChBD2_{PF\text{-}ChiA}$; Nakamura *et al.*, 2005) and two active (catalytic) domains ($AD1_{PF\text{-}ChiA}$ and $AD2_{PF\text{-}ChiA}$). Both catalytic domains are classified into family 18. Interestingly, this PF-ChiA exhibits hydrolytic activity toward not only colloidal but also crystalline (β/α) chitins at high temperature (Oku & Ishikawa, 2006).

Here, we report the first crystal structure of the active (catalytic) domain ($AD2_{PF\text{-}ChiA}$) of a hyperthemophilic archaeal chitinase at 1.5 Å resolution and discuss the structural comparisons with other family 18 chitinases.

2. Materials and methods

The construction of the expression plasmid has been described previously (Mine *et al.*, 2006). In this construct, $AD2_{PF\text{-}ChiA}$ was

expressed with an N-terminal thioredoxin-His_6 tag (Fig. 1), the fusion tag being removed by proteolytic cleavage with PreScission Protease (Amersham Biosciences; Mine *et al.*, 2006). *Escherichia coli* cells harbouring the expression plasmid were cultivated in a modified M9 medium containing selenomethionine and inhibitors of methionine biosynthesis (Doublié, 1997) to produce a selenomethionine derivative of $AD2_{PF\text{-}ChiA}$. The selenomethionine derivative of $AD2_{PF\text{-}ChiA}$ was purified by the same method for the native protein (Mine *et al.*,

Table 1
Summary of the crystallographic data.

Values in parentheses are for the highest resolution shell.

	Native†	Peak	Edge	Low remote	High remote
Data-collection statistics					
X-ray source	BL44XU, SPring-8	BL38B1, SPring-8	BL38B1, SPring-8	BL38B1, SPring-8	BL38B1, SPring-8
Wavelength (Å)	0.7	0.97915	0.97934	0.99506	0.96411
Space group	$P2_12_12_1$	$P2_12_12_1$			
Unit-cell parameters (Å)	a = 90.0, b = 92.8, c = 107.2	a = 89.9, b = 92.6, c = 107.2			
Resolution range (Å)	50–1.50 (1.55–1.50)	50–2.00 (2.07–2.00)	50–2.00 (2.07–2.00)	50–2.00 (2.07–2.00)	50–2.00 (2.07–2.00)
R_{sym}‡ (%)	10.7 (26.6)	8.6 (15.4)	6.7 (14.0)	6.7 (14.9)	7.3 (17.6)
$I/\sigma(I)$	18.0	20.0	19.2	19.0	15.8
Total reflections	1109463	433225	435356	415388	433555
Unique reflections	142710 (14039)	58665	58691	56051	61306
Redundancy	7.8 (5.9)	7.4 (6.7)	7.4 (6.6)	7.4 (5.8)	7.4 (7.1)
Completeness (%)	99.5 (98.8)	96.1 (60.4)	96.0 (59.5)	91.6 (14.5)	100 (100)
B factor of data from Wilson plot (Å^2)	14.8				
Se atoms found/total		14/14			
Average figure of merit§		0.66			
Refinement statistics					
Resolution range (Å)	25.2–1.50 (1.59–1.50)				
No. of reflections	142675 (22020)				
R_{cryst}¶ (%)/R_{free}†† (%)	16.8 (20.2)/18.0 (22.3)				
R.m.s.d. bond lengths (Å)	0.005				
R.m.s.d. angles (°)	1.3				
Polypeptide chains in the asymmetric unit	2				
Matthews coefficient (Å^3 Da^{-1})	3.20				
Protein atoms	4768				
Average B factor (Å^2)	14.9				
Water molecules	650				
Average B factor (Å^2)	29.6				
Sulfate ion	1				
Glycerol molecules	6				
Ramachandran plot‡‡ (%)					
Favoured	90.8				
Allowed	8.8				
Disallowed§§	0.4				

† Data-collection statistics for the native crystal are taken from Mine *et al.* (2006). ‡ $R_{sym} = \sum_{hkl}\sum_i I_i(hkl) - \langle I(hkl)\rangle|/\sum_{hkl}\sum_i I_i(hkl)$, where $I_i(hkl)$ is the ith intensity measurement of reflection hkl, including symmetry-related reflections, and $\langle I(hkl)\rangle$ is the average. § Figure of merit = $|F(hkl)_{best}|/F(hkl)$. ¶ $R_{cryst} = \sum ||F_o| - |F_c||/\sum |F_c|$, where F_o and F_c are the observed and calculated structure-factor amplitudes, respectively. †† R_{free} was calculated using a randomly selected 5% of the data set that was omitted through all stages of refinement. ‡‡ The Ramachandran plot was obtained for all residues other than Gly and Pro. §§ The disallowed conformation is found for Tyr590; nevertheless, the electron-density map around Tyr590 is clear and is shown in Fig. 7.

Figure 1
Schematic representation of the fusion protein thioredoxin-His_6tag-PS-$AD2_{PF\text{-}ChiA}$. PreScission protease recognizes a subset of sequences which includes the PS sequence LEVFQGP (underlined), cleaving between the Q and G residues.

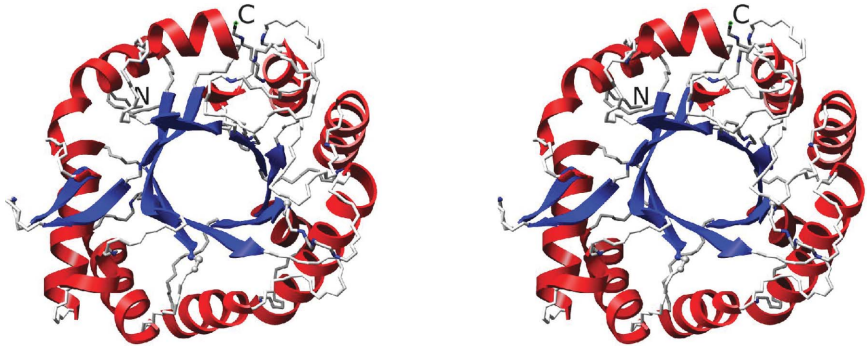

Figure 2
Overall structure of $AD2_{PF\text{-}ChiA}$. The α-helices and β-strands are shown in red and blue, respectively.

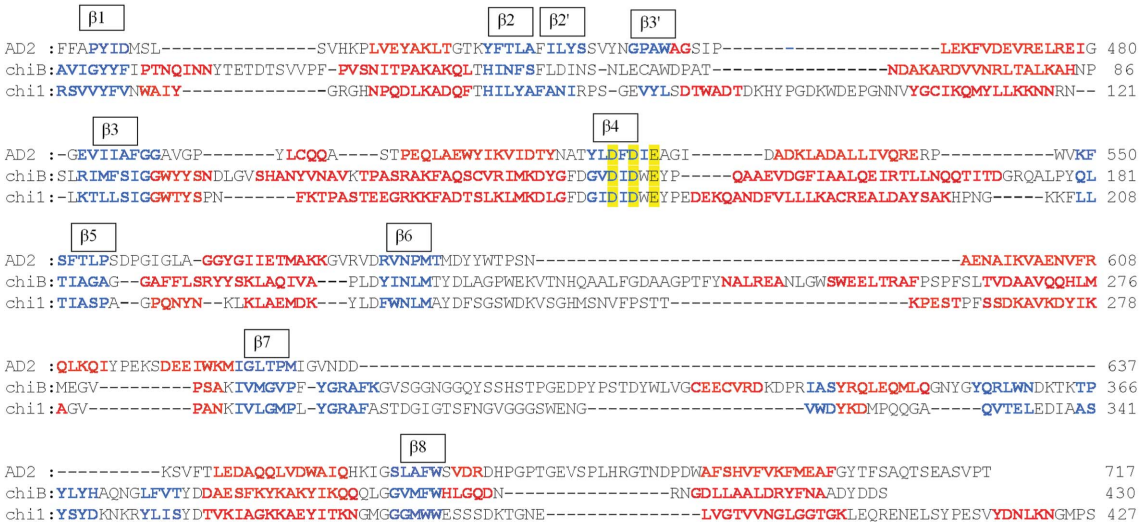

Figure 3
Multiple alignments of the protein sequences were performed based on the three-dimensional structure. Red and blue characters indicate α-helices and β-strands, respectively. The D_2XD_3XE motif is indicated in yellow.

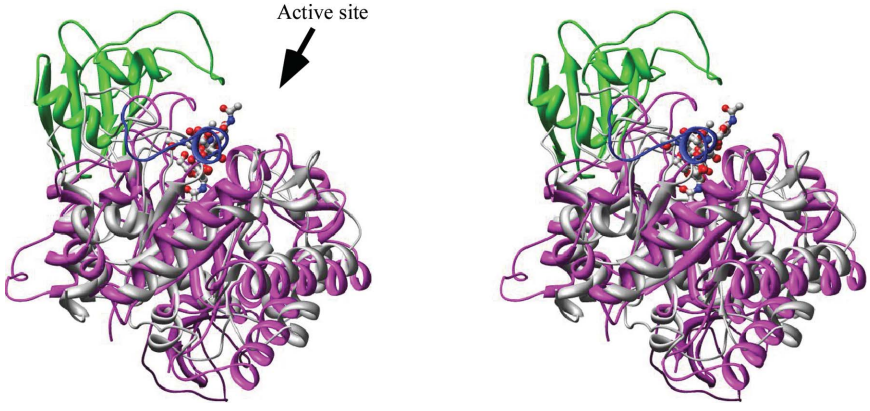

Figure 4
Stereoview of the overlaid structure of $AD2_{PF\text{-}ChiA}$ (grey) and the complex of chitinase B with $(GlcNAc)_6$ (magenta). The porch loop and the α/β domain of chitinase B are shown in blue and green, respectively, and GlcNAc is shown in ball-and-stick representation. The β-strands in TIM-barrel fold were used for the superposition (the r.m.s. deviation is 1.26 Å between backbone atoms for 46 residues).

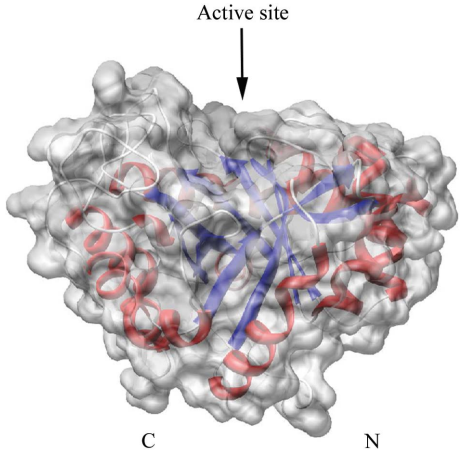

Figure 5
Surface representation of $AD2_{PF\text{-}ChiA}$. The active-site cleft is indicated by an arrow. The α-helices and the β-strands are shown in red and blue, respectively. N and C indicate the N- and C-termini, respectively.

2006). In brief, the fusion protein was isolated by Ni^{2+}-chelating chromatography followed by removal of the fusion tag. The final purification step was anion-exchange chromatography using a HiTrap-Q column (Amersham Biosciences). Crystallization of the selenomethionine derivative of $AD2_{PF\text{-}ChiA}$ was performed using the same method as used for the native protein (Mine *et al.*, 2006).

Diffraction data for the selenomethionine derivative were collected at BL38B1, SPring-8 (Harima, Japan) and processed using *HKL*-2000 (Otwinowski & Minor, 1997). Selenium sites were searched for with *SOLVE* (Terwilliger & Berendzen, 1999) and all 14 sites were found in the asymmetric unit. Initial phase sets were calculated by the MAD method and improved by density modification with *RESOLVE* (Terwilliger & Berendzen, 1999). The model of a single polypeptide was built in the experimental electron-density map using *O* (Jones *et al.*, 1991). This initial model was used to phase a higher resolution native data set (1.5 Å; Mine *et al.*, 2006) using *MOLREP* from the *CCP*4 suite (Collaborative Computational Project, Number 4, 1994). The native crystal contained two polypeptides in the asymmetric unit. Refinement was performed using *CNS* (Brünger *et al.*, 1998). Stereochemical analysis and structural

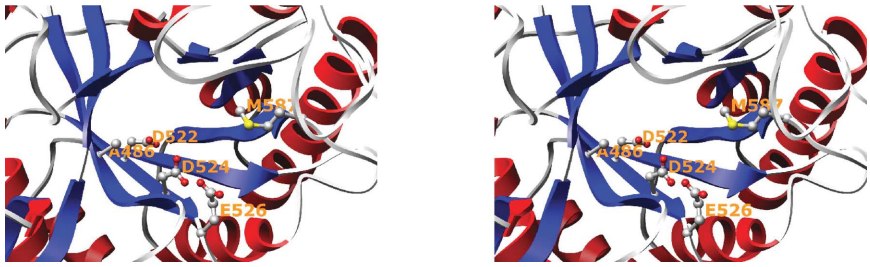

Figure 6
Close-up view of the active site containing the conserved residues in family 18 chitinases. The side chains of Asp522, Asp524 and Glu526, which are important for catalysis, are shown. In addition, Ala486 and Met587, which correspond to Ser and Tyr in other chitinases, are also shown.

comparisons were carried out using *PROCHECK* (Laskowski *et al.*, 1993) and *CHIMERA* (Pettersen *et al.*, 2004), respectively. The diffraction data statistics and the crystallographic refinement statistics are summarized in Table 1.

3. Results and discussion

The structure of $AD2_{PF\text{-}ChiA}$ was solved at 1.5 Å resolution. The polypeptide chain was successfully traced from the N-terminal Asn409 to Phe706. At the C-terminus, 11 amino acids could not be traced owing to a lack of electron density. The overall structure of $AD2_{PF\text{-}ChiA}$ is a TIM-barrel $(\beta/\alpha)_8$-fold with a tunnel-like active site (Fig. 2) that is a common feature of exo-chitinases (Davies & Henrissat, 1995; Spezio *et al.*, 1993; Rouvinen *et al.*, 1990). Chitinase B from *S. marcescens* (PDB code 1e15) and chitinase 1 from *Coccidioides immitis* (PDB code 1d2k) were retrieved from the family 18 chitinases with the highest *Z* scores (19.8 and 18.8, respectively) using the *DALI* server (http://www.ebi.ac.uk/dali/; Fig. 3). $AD2_{PF\text{-}ChiA}$ has shorter $\beta1$ and $\beta7$ strands than chitinases B and 1. Moreover, $AD2_{PF\text{-}ChiA}$ lacks an insertion domain between the $\beta7$ and $\beta8$ strands. Chitinase B and chitinase 1 contain an additional small $\alpha + \beta$ insertion domain which provides one side of a deep substrate-binding cleft at the top of the catalytic $(\beta/\alpha)_8$ domain (Fig. 4). Therefore, the substrate-binding cleft of $AD2_{PF\text{-}ChiA}$ is not as deep as those of chitinases B and 1. Another notable deletion in $AD2_{PF\text{-}ChiA}$ is the 'porch loop' between $\beta3$ and $\beta4$. The porch loop is a barrier that is formed by the short helix and loop in chitinase B (van Aalten *et al.*, 2001). In chitinase B, this loop prevents binding of substrate (GlcNAc) extending longer than three units from the scissile glycosidic bond (Fig. 4). The absence of the porch loop in $AD2_{PF\text{-}ChiA}$ indicates that the substrate-binding cleft is open on both sides of the active site (Fig. 5). Thus, the active-site cleft of $AD2_{PF\text{-}ChiA}$ may accommodate substrates longer than those of chitinase B (Fig. 4).

It has been suggested that the conserved amino-acid sequence (D_2XD_3XE motif) that spans the $\beta4$ strand plays an important role in the catalytic mechanism of family 18 chitinases (Fig. 6; Watanabe *et al.*, 1993, 1994). The catalytic Glu526 is located at the end of the $\beta4$ strand and the two conserved aspartic acid residues [Asp522 (D_2) and Asp524 (D_3)] are linearly aligned in the active-site core (Fig. 6). Structural studies of chitinase B–substrate complexes have shown that the functionality of Asp142 (D_3) during catalysis depends on the presence of Ser93 and that Tyr214 interacts with the distorted *N*-acetyl group of GlcNAc (van Aalten *et al.*, 2001). However, these residues, Ser93 and Tyr214 in chitinase B, are not conserved in $AD2_{PF\text{-}ChiA}$, the corresponding residues being Ala486 and Met587. These observations indicate that the chitin-recognition mechanism of $AD2_{PF\text{-}ChiA}$ must be different from that of chitinase B. PF-ChiA possesses a unique feature in that it catalyzes the hydrolysis of both colloidal and crystalline (β/α) chitins. This may arise from the catalytic mechanism of PF-ChiA, which is uncommon in family 18 chitinases. In addition, comparison of the $AD2_{PF\text{-}ChiA}$ structure with that of chitinase B suggests that $AD2_{PF\text{-}ChiA}$ may be an endo-type chitinase. $AD2_{PF\text{-}ChiA}$ has a groove-like cleft that is typical of endo-enzymes, whereas chitinase B is an exo-type chitinase with a tunnel-like cleft. To clarify this issue, we are now attempting to solve the structure of $AD2_{PF\text{-}ChiA}$ complexed with its substrate.

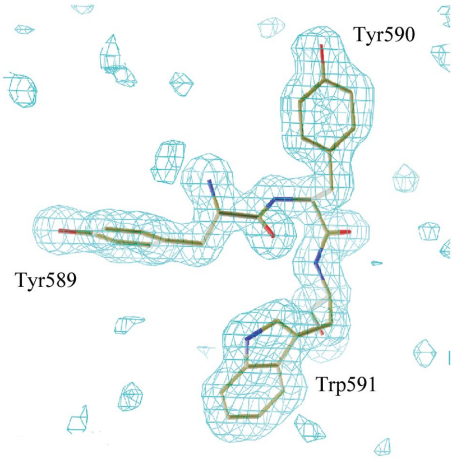

Figure 7
The conformation around Tyr590. The electron density shows a σ_A-weighted $F_o - F_c$ map at the 3.0σ level when three amino-acid residues (Tyr589, Tyr590 and Trp591) were removed from the structure-factor calculation.

We thank Dr H. Matsumura (Osaka University) for helpful advice on X-ray diffraction analysis. We also thank Ms C. Yoshikawa-Kageyama for performing part of the protein-purification and molecular-biological work. This work was supported by the National Project on Protein Structural and Functional Analyses. The X-ray diffraction experiments were carried out with the approval of the Japan Synchrotron Radiation Research Institute (proposal No. 2005AC05A44XU-7201-N).

References

Aalten, D. M. van, Komander, D., Synstad, B., Gaseidnes, S., Peter, M. G. & Eijsink, V. G. (2001). *Proc. Natl Acad. Sci. USA*, **98**, 8979–8984.
Aalten, D. M. van, Synstad, B., Brurberg, M. B., Hough, E., Riize, B. W., Eijsink, V. G. & Wierenga, R. K. (2000). *Proc. Natl Acad. Sci. USA*, **97**, 5842–5847.
Brünger, A. T., Adams, P. D., Clore, G. M., DeLano, W. L, Gros, P., Grosse-Kunstleve, R. W., Jiang, J.-S., Kuszewski, J., Nilges, M., Pannu, N. S., Read, R. J., Rice, L. M., Simonson, T. & Warren, G. L. (1998). *Acta Cryst.* D**54**, 905–921.

Collaborative Computational Project, Number 4 (1994). *Acta Cryst.* D**50**, 760–763.
Davies, G. & Henrissat, B. (1995). *Structure*, **3**, 853–859.
Doublié, S. (1997). *Methods Enzymol.* **276**, 523–530.
Henrissat, B. (1991). *Biochem. J.* **280**, 309–316.
Henrissat, B. & Davies, G. (1997). *Curr. Opin. Struct. Biol.* **7**, 637–644.
Jones, T. A., Zou, J.-Y., Cowan, S. W. & Kjeldgaard, M. (1991). *Acta Cryst.* A**47**, 110–119.
Laskowski, R. A., Moss, D. S. & Thornton, J. M. (1993). *J. Mol. Biol.* **231**, 1049–1067.
Matsumoto, T., Nonaka, T., Hashimoto, M., Watanabe, T. & Mitsui, Y. (1999). *Proc. Jpn Acad.* **75**, 269–274.
Mine, S., Nakamura, T., Hirata, K., Ishikawa, K., Hagihara, Y. & Uegaki, K. (2006). *Acta Cryst.* F**62**, 791–793.
Nakamura, T., Ishikawa, K., Hagihara, Y., Oku, T., Nakagawa, A., Inoue, T., Ataka, M. & Uegaki, K. (2005). *Acta Cryst.* F**61**, 476–478.
Oku, T. & Ishikawa, K. (2006). *Biosci. Biotechnol. Biochem.* **70**, 1969–1701.
Otwinowski, Z. & Minor, W. (1997). *Methods Enzymol.* **276**, 307–326.
Perrakis, A., Tews, I., Dauter, Z., Oppenheim, A. B., Chet, I., Wilson, K. S. & Vorgias, C. E. (1994). *Structure*, **2**, 1169–1180.
Pettersen, E. F., Goddard, T. D., Huang, C. C., Couch, G. S., Greenblatt, D. M., Meng, E. C. & Ferrin, T. E. (2004). *J. Comput. Chem.* **25**, 1605–1612.
Rouvinen, J., Bergfors, T., Teeri, T., Knowles, J. K. & Jones, T. A. (1990). *Science*, **249**, 380–386.
Spezio, M., Wilson, D. B. & Karplus, P. A. (1993). *Biochemistry*, **32**, 9906–9916.
Suzuki, K., Taiyoji, M., Sugawara, N., Nikaidou, N., Henrissat, B. & Watanabe, T. (1999). *Biochem. J.* **343**, 587–596.
Terwilliger, T. C. & Berendzen, J. (1999). *Acta Cryst.* D**55**, 849–861.
Terwisscha van Scheltinga, A. C., Hennig, M. & Dijkstra, B. W. (1996). *J. Mol. Biol.* **262**, 243–257.
Watanabe, T., Kobori, K., Miyashita, K., Fujii, T., Sakai, H., Uchida, M. & Tanaka, H. (1993). *J. Biol. Chem.* **268**, 18567–18572.
Watanabe, T., Uchida, M., Kobori, K. & Tanaka, H. (1994). *Biosci. Biotechnol. Biochem.* **58**, 2283–2285.